Propagation in Optical Fibres

HTE - 29.01.2013

1. Basics

For sinusoidal variations, the basic relation between speed of light, denoted by c frequency (of light) denoted by f and wavelength (of light) denoted by λ is

$$c = f\lambda \tag{1.1}$$

where $c = 2.997925\times10^{8}\ \mathrm{m/s} \approx 3\times10^{8}\ \mathrm{m/s}$ in vacuum (free space), i.e. in atmosphere free environment. Depending on the refractive index of the medium, n, the speed of light and the related quantities will change as

$$c_n = \frac{c}{n} \quad , \quad \lambda_n = \frac{\lambda}{n} \quad , \quad k_n = kn = \frac{2n\pi}{\lambda} = \frac{2\pi}{\lambda_n}$$

c : speed of light in free space , c_n : speed of light in medium with refractive index n

λ : wavelength of light in free space , λ_n : wavelength of light in medium with refractive index n

k : wave number in free space , k_n : wave number in medium with refractive index n (1.2)

The implication in (1.2) is that if the refractive index of the medium is $n = 1$, then the speed of light, wavelength of light and the associated wave number will remain as that of vacuum, that is the parameters without any index. But if $n \neq 1$, then $c_n < c$, $\lambda_n < \lambda$ and $k_n > k$, since in vacuum, $n = 1$ and in other mediums $n > 1$, for instance, $n = 1.33$ in water, $n = 1.5$ in glass, $n = 2.42$ in diamond. Another implication of (1.2) is that when light changes the medium of propagation, its speed, its wavelength and the wave number change but its frequency (i.e. the number of cycles it makes per unit time) remains the same such that $c = f\lambda$ is always satisfied. The refractive index property is related to the dielectric characteristics of the medium and is also measured by the dielectric constant, relative permittivity, as we shall see later.

It is worth noting that refractive index may change according to spatial coordinates, even with time (temporal coordinate). Being aware of such characteristics allows us to guide light and a medium, thus achieve communication using light frequencies as carriers. It is important to realize that optical frequencies are quite high, for instance at a wavelength of $\lambda = 1\ \mu\mathrm{m}$, the frequency becomes

$$f = \frac{c}{\lambda} = \frac{3\times10^{8}\ \mathrm{m/s}}{1\ \mu\mathrm{m}} = 3\times10^{14}\ \mathrm{Hz} = 300\ \mathrm{THz} \tag{1.3}$$

Hence it is reasonable to assume that we can place, multiplex (in FDM sense) a lot of message signals onto such high frequency carriers. It is customary to speak in terms of wavelengths rather than frequencies for the optical range.

1. 1 Simple Laws of Reflection, Refraction, Principle of Total Reflection

By taking a simple two dimensional geometry, we illustrate in Fig. 1.1, an optical ray incident on a boundary where there occurs a change in the refractive index and how it is reflected and refracted.

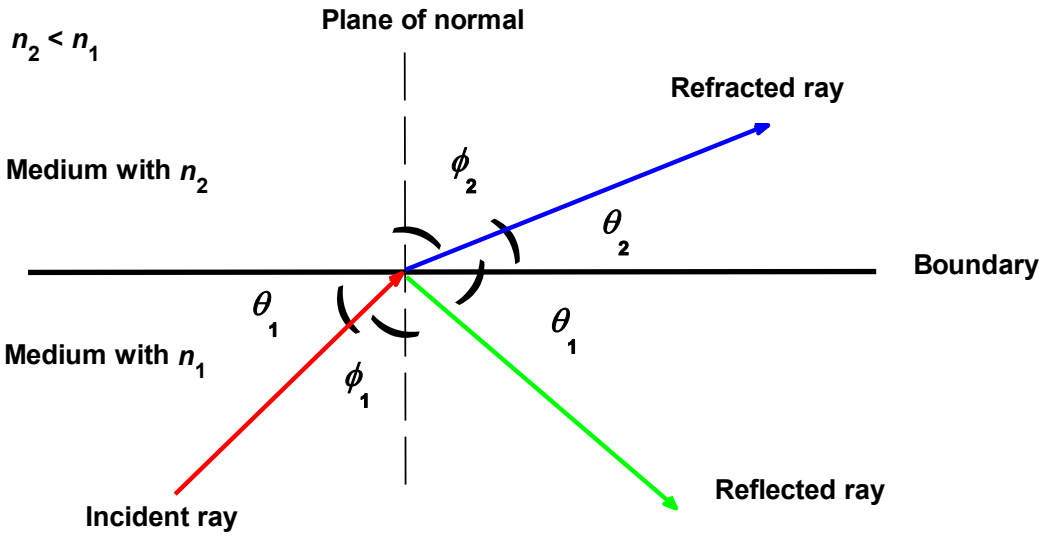

Fig. 1.1 Illustration of simple two dimensional geometry for incident, reflected and refracted rays.

As seen from Fig. 1.1, when a ray is incident upon a boundary where there is a refractive index change from n_1 to n_2, there is refraction as well as reflection. The amount of reflection and refraction is related to the individual refractive indices of the two mediums. Since we have arranged that $n_2 < n_1$, then $\phi_1 < \phi_2$, and according to Snell's law, these angles are connected as follows

$$n_1 \sin(\phi_1) = n_2 \sin(\phi_2) \tag{1.4}$$

Furthermore, the angle of incidence and the angle of reflection are the same, i.e. they are both θ_1 as shown in Fig. 1.1.

From (1.4), we deduce that there will be an angle of ϕ_1 such that $\phi_2 = \pi/2$, then

$$n_1 \sin(\phi_1) = n_2 \sin\left(\frac{\pi}{2}\right) = n_2 \tag{1.5}$$

At this point, we let $\phi_1 \rightarrow \phi_c$ and call ϕ_c the critical angle, hence

$$\sin(\phi_c) = \frac{n_2}{n_1} \quad \text{or} \quad \phi_c = \sin^{-1}\left(\frac{n_2}{n_1}\right) = \text{asin}\left(\frac{n_2}{n_1}\right) \tag{1.6}$$

Under the circumstances that ϕ_1 reaches ϕ_c, the refracted component will vanish and there will be total reflection as shown in Fig. 1.2. Note that since $\theta_1 + \phi_1 = \pi/2$, the condition in (1.6) can also be expressed as

$$\cos(\theta_c) = \frac{n_2}{n_1} \quad \text{or} \quad \theta_c = \cos^{-1}\left(\frac{n_2}{n_1}\right) = \text{acos}\left(\frac{n_2}{n_1}\right) \tag{1.7}$$

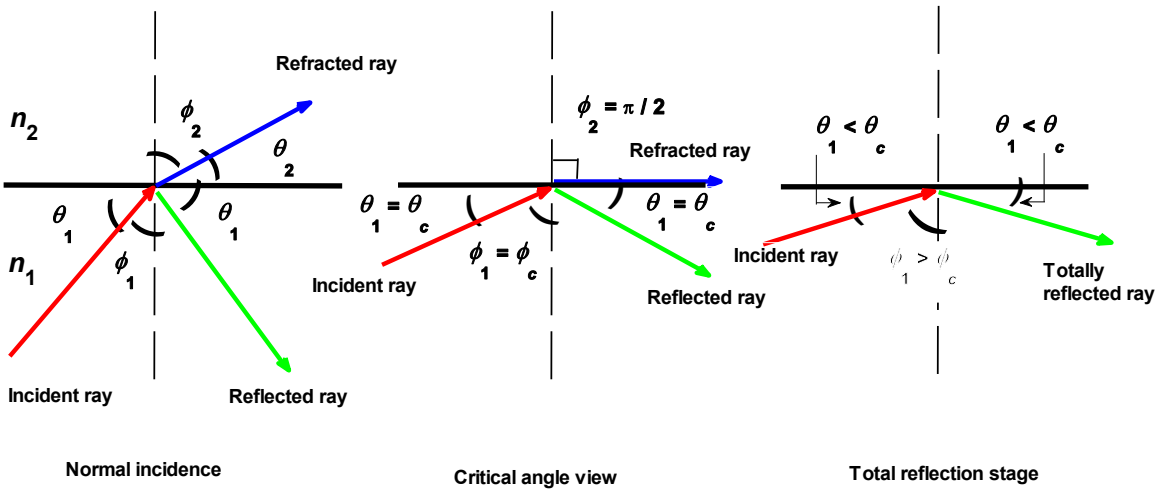

Fig. 1.2 Illustration of reaching the critical angle and total reflection stage.

Assuming that propagation of light can be represented in terms of ray tracing as given in Figs. 1.1 and 1.2, the above total reflection phenomena is exactly the principle of light guidance in optical fibres.

Exercise 1. 1 : Consider a boundary between air (vacuum) and water. Find the critical angles ϕ_c and θ_c for total reflection to occur. Discuss if total reflection is possible both ways, i.e. when the incident ray is on the side of air medium and when the incident ray is on the side of water medium. Make the necessary plots and indicate the necessary angles.

Comments on the total reflection phenomena shown in Fig. 1.2

a) It is obvious then when $n_1 < n_2$, then it is impossible to reach a stage of critical angle and total reflection. In this case mostly refraction will take place.
b) Light propagation can be studied both in terms or rays and waves. When we do wave analysis, then we find that even after the critical angle stage, refraction (or energy loss due to refraction) is possible due to electromagnetic tunnelling, depending on how much the field extends into the other medium beyond the boundary.
c) In real life, we have a three dimensional situation and the boundary is not a flat surface. Despite this however, Fig. 1.1 provides the basic principle of reflection and refraction mechanisms.

2. Optical Fibres

2.1 Mechanical Construction of Optical Fibres

An optical fibre cable is a cylindrical shaped closed medium that guides or carries light in the form of electromagnetic waves. The mechanical construction of the optical fibre is shown in Fig. 2.1. Due to the existence of boundary conditions set by the physical dimensions, only those waves, called modes, are allowed to propagate. This propagation is mostly confined to the core region. The refractive index difference between the core and the cladding provides the necessary guidance of the electromagnetic waves or the total internal reflection mechanism along the fibre propagation axis.

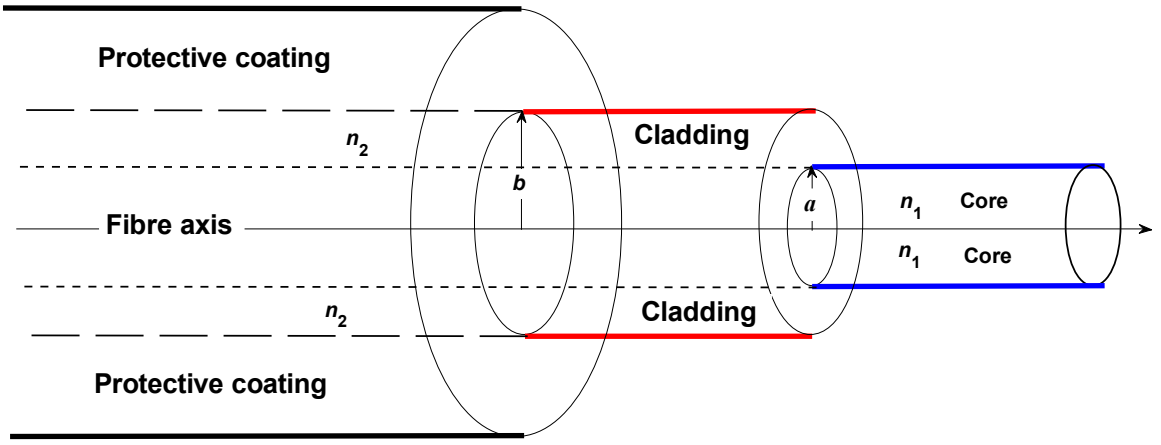

Fig. 2.1 Mechanical construction of a fibre cable.

We classify three types of fibre, depending on core radius (or diameter), i.e., a, refractive index profile in the core, i.e. n_1. These are step index multimode, graded index multimode and step index single mode fibres, as illustrated in Fig. 2.2.

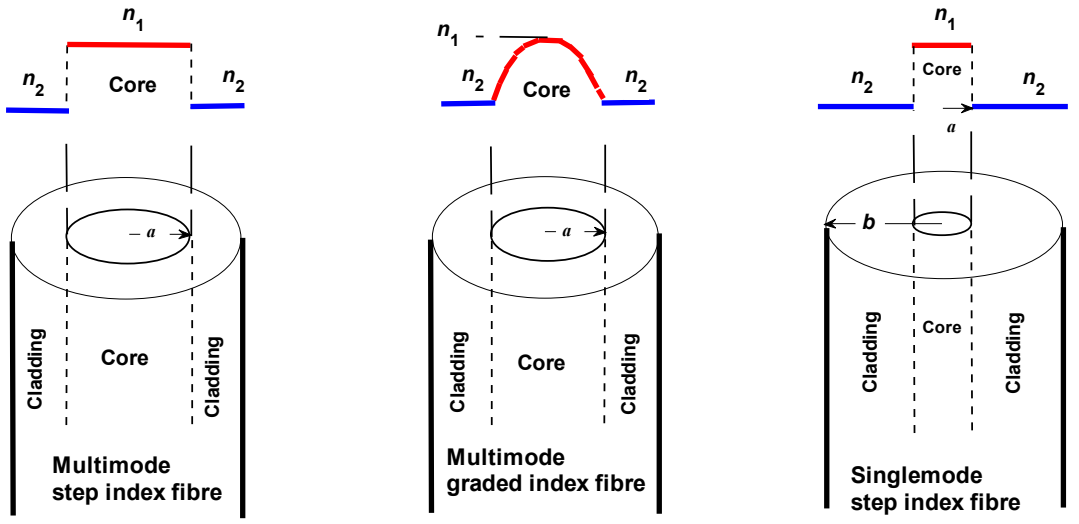

Fig. 2.2 Types of fibres.

As the names given in Fig. 2.2 imply, many modes propagate in multimode fibres, since many modes satisfy the propagation conditions, this causes dispersion, because the time it takes for each mode to traverse the fibre length is different. This is balanced to a certain extent in graded index fibres. On the other hand, single mode fibres are constructed so that they transmit only the fundamental mode,

called HE_{11}, thus these fibres do not suffer from multimode dispersion. Almost 100 % of the fibres used in public communication facilities are single mode fibres (single mode fibres have always step refractive index profile).

The physical core and cladding dimensions (radius or diameter) are more or less standardized as follows

a) The cladding diameter is always, $2b = 125\ \mu\text{m}$.
b) The core diameter in multimode fibres is $2a = 50\ \mu\text{m}$.
c) The core diameter in single mode fibres may vary $2a = 2\ \mu\text{m} \rightarrow 10\ \mu\text{m}$. As will be seen later the single mode property is achieved by arranging the parameters of core radius, wavelength of operation and the refractive index difference between core and cladding, i.e. between n_1 and n_2.

2.2 Numerical Aperture

Now based on the simple rules of reflection and refraction depicted in Fig. 1.1 and 1.2, we try to determine, the ray collecting cone of the fibre front face, i.e. fibre entrance. So this is finding the maximum incidence angles of rays, which will propagate in fibre. Fig. 2.3 shows the associated two dimensional view of this situation for a simple multimode step index fibre.

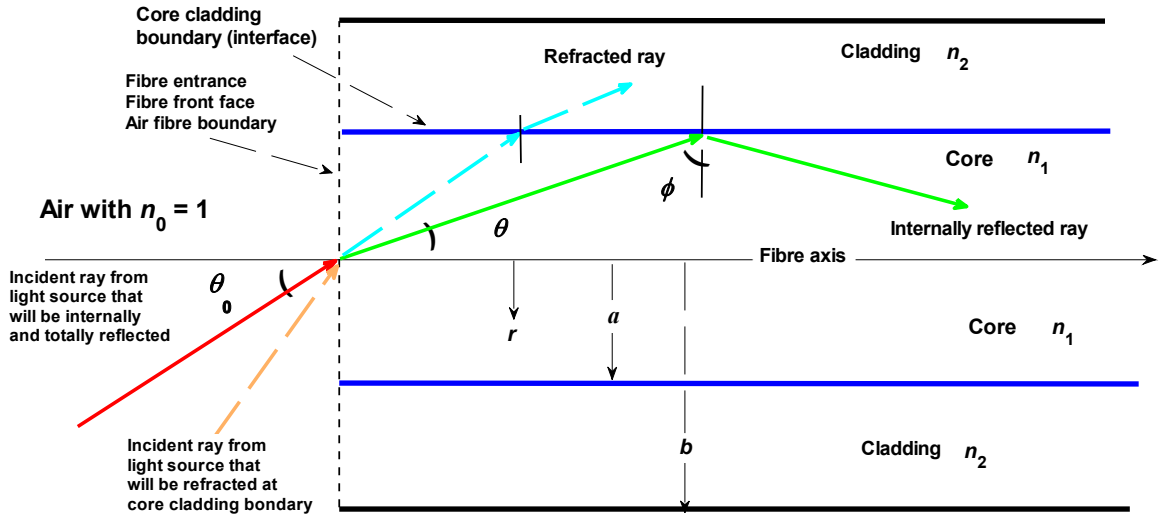

Fig. 2.3 View of fibre end face for calculation of numerical aperture.

Looking at Fig. 2.3, we note that the reflection and the refraction phenomena encountered on the core cladding boundary (interface) is exactly the same as the one in Figs. 1.1 and 1.2. Hence from (1.6), we write the for the condition of an incident ray from the light source to be totally internally reflected from the core cladding boundary as

$$\sin(\phi_c) = \frac{n_2}{n_1} \tag{2.1}$$

where ϕ_c is the critical value of the angle ϕ which means that for total internal reflection to take place, the minimum value that can be taken up by ϕ is ϕ_c. So total internal reflection will take place

provided that $\phi \geq \phi_c$. Rearranging (2.1) and relating the result to the angle θ by keeping in mind that $\phi + \theta = \pi/2$, we get

$$\sin^2(\phi_c) = \frac{n_2^2}{n_1^2} \quad , \quad 1 - \sin^2(\phi_c) = \frac{n_1^2 - n_2^2}{n_1^2} = \sin^2(\theta_c)$$
$$\cos(\theta_c) = \frac{n_2}{n_1} \quad , \quad \theta_c = \cos^{-1}\left(\frac{n_2}{n_1}\right) = a\cos\left(\frac{n_2}{n_1}\right) \tag{2.2}$$

Thus similar to discussion for ϕ, we can say that, total internal reflection will take place if $\theta \leq \theta_c$. Using the Snell's law, we can also relate everything to the angle of fibre entrance, θ_0 as

$$n_0 \sin(\theta_0) = n_1 \sin(\theta) = \sin(\theta_0) \quad , \quad n_0 = 1$$
$$\sin(\theta_{0c}) = n_1 \sin(\theta_c) \tag{2.3}$$

Using (2.2), we define the acceptance angle called the numerical aperture (NA) as sine of the maximum angle subtended by a ray at fibre entrance, i.e. $\sin(\theta_{0c})$ or alternatively as the product of the core refractive index, n_1 and the sine of maximum angle of a refracted ray at fibre entrance, hence NA will be given by

$$\text{NA} = \sin(\theta_{0c}) = n_1 \sin(\theta_c) = \left(n_1^2 - n_2^2\right)^{0.5} \tag{2.4}$$

It is important to realize that NA is solely determined by the total internal reflection conditions at the core cladding boundary. Otherwise rays with any value of θ_0 will enter (refract into) the fibre, since $n_1 > n_0 = 1$.

As can be seen (2.4) is in the form of refractive index difference between core and cladding. In other words, the principle of light guidance in fibres is based on the (minute) refractive index difference between core and cladding, rather than the absolute values of n_1 and n_2. For this reason we define the following (normalized) refractive index difference term

$$\Delta = \frac{n_1^2 - n_2^2}{2n_1^2} \simeq \frac{n_1 - n_2}{n_1} \ll 1 \quad , \quad \Delta n_1 = n_1 - n_2 \quad , \quad 2n_1 \simeq n_1 + n_2 \tag{2.5}$$

In terms of Δ, NA will become

$$\text{NA} = \left[(n_1 - n_2)(n_1 + n_2)\right]^{0.5} = n_1\sqrt{2\Delta} \tag{2.6}$$

It is important to summarize the conditions of total internal reflection and refraction in a step fibre as follows

$$\begin{aligned} &\text{If} \quad \phi \geq \phi_c \text{ or } \theta \leq \theta_c \text{ or } \theta_0 \leq \theta_{0c} \quad \text{total internal reflection ito the core} \\ &\qquad\qquad\qquad\qquad\qquad\qquad\qquad\qquad\qquad\quad \text{or propagation along fibre axis} \\ &\text{If} \quad \phi \leq \phi_c \text{ or } \theta \geq \theta_c \text{ or } \theta_0 \geq \theta_{0c} \quad \text{refraction out to cladding} \end{aligned} \tag{2.7}$$

Example 2.1 : A step index optical fibre has a core diameter is large enough so that the ray theory is considered applicable. In this fibre, $n_1 = 1.5$ and $n_2 = 1.47$. Determine the followings

a) The critical angle at core cladding boundary for total internal reflection to occur, i.e. ϕ_c .
b) NA of the fibre.
c) The acceptance angle, θ_{0c} at the air fibre boundary.

Solution :

a) From (2.1), the angle at core cladding boundary for total internal reflection to occur is

$$\phi_c = \sin^{-1}\left(\frac{n_2}{n_1}\right) = \sin^{-1}\left(\frac{1.47}{1.5}\right) = 78.5^0 \tag{2.8}$$

b) From (2.4), NA is

$$\mathrm{NA} = \left(n_1^2 - n_2^1\right)^{0.5} = \left(1.5^2 - 1.47^2\right)^{0.5} = 0.3 \tag{2.9}$$

c) From (2.4), the acceptance angle, θ_{0c} at the air fibre boundary is

$$\theta_{0c} = \sin^{-1}\left(\mathrm{NA}\right) = 17.4^0 \tag{2.10}$$

As seen in this numeric example, the refractive index difference between the core and the cladding is indeed small (minute).

Exercise 2.1 : Examine the dependence of ϕ_c , NA and θ_{0c} on n_1 and n_2 in a step index fibre. Comment whether the larger or smaller values of ϕ_c , NA and θ_{0c} would be useful.

The above analysis is quite useful to given an insight into propagation of rays in a fibre. But we should not forget that ray theory is applicable if the dimensions of the physical objects are much larger than the wavelength. For instance in the above case, where the (multimode) step index fibre was considered, the fibre core diameter is 50 $\mu\mathrm{m}$, hence compared with a wavelength of $\lambda = 1$, we can safely say that ray theory is applicable. But in other cases, we certainly have to use wave or mode theory which is applicable independent of dimensions of the physical objects present on the way of propagation. In particular, we need to see how we can approach the single mode limit. We do this in the next section.

3. Mode Theory (Modal Analysis)

For this analysis, convenient form of Maxwell's equations is required. Because of the cylindrical geometry of the fibre, we use cylindrical coordinates, where the respective coordinates will be $r,\ \phi,\ \mathrm{z}$ as shown in Fig. 3.1.

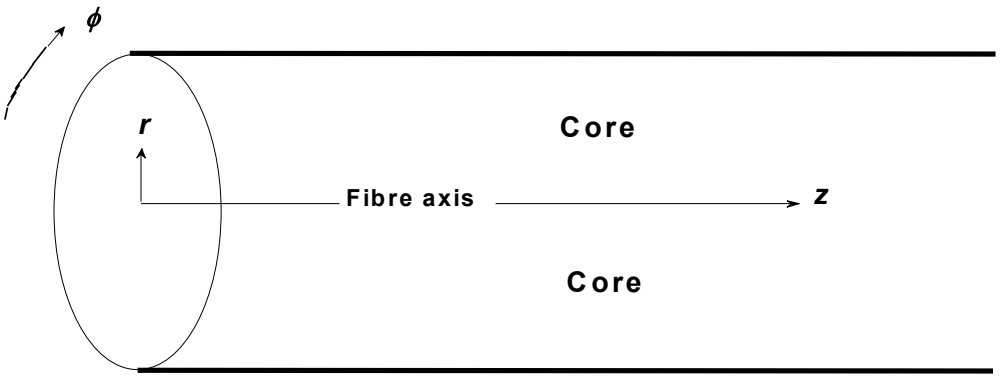

Fig. 3.1 Coordinate axes in a fibre.

In (3.1), we find the relevant Maxwell's equations.

$$\begin{aligned}
&\text{Curl of } \mathbf{E}: \quad \nabla \times \mathbf{E} = -\frac{\partial \mu \mathbf{H}}{\partial t} \\
&\text{Curl of } \mathbf{H}: \quad \nabla \times \mathbf{H} = \frac{\partial \varepsilon \mathbf{E}}{\partial t} \\
&\text{Div of } \mathbf{E}: \quad \nabla \cdot \mathbf{E} = 0 \quad , \quad \text{Div of } \mathbf{H}: \quad \nabla \cdot \mathbf{H} = 0
\end{aligned} \tag{3.1}$$

$\mathbf{E}$ and $\mathbf{H}$ are electric and magnetic field vectors, t indicates time. μ and ε stand for the permeability and permittivity of the medium so that they represent the magnetic and electrical properties of the medium. μ and ε are further expanded as given below in (3.2)

$$\begin{aligned}
\mu = \mu_r \mu_0 \qquad & \mu_r : \text{Relative permeability of medium} \\
& \mu_0 : \text{Permeability of free space (vacuum)} \\
\varepsilon = \varepsilon_r \varepsilon_0 \qquad & \varepsilon_r : \text{Relative permitivity of medium} \\
& \varepsilon_0 : \text{Permitivity of free space (vacuum)}
\end{aligned} \tag{3.2}$$

The speed of light in vacuum and in other mediums, the wave number in free space and in other mediums are further related to the quantities of (3.2) as follows

Free space: $c = \dfrac{1}{\sqrt{\mu_0 \varepsilon_0}} = \lambda f = \lambda \dfrac{\omega}{2\pi} = \dfrac{\omega}{k}$ c : speed of light in free space

λ : wavelength of light in free space

f : frequency of light in free space

ω : angular frequency of light in free space

In a medium with $\varepsilon_1 = \varepsilon_{r_1}\varepsilon_0$, $\mu_1 = \mu_{r_1}\mu_0 = \mu_0$, $\mu_{r_1} = 1$

$$c_1 = \frac{1}{\sqrt{\mu_1 \varepsilon_1}} = \frac{1}{\sqrt{\mu_0 \varepsilon_1}} = \frac{1}{\sqrt{\mu_0 \varepsilon_{r_1} \varepsilon_0}} = \lambda_1 f = \lambda_1 \frac{w}{2\pi} = \frac{w}{k_1} = \frac{c}{n_1} = \frac{1}{n_1 \sqrt{\mu_0 \varepsilon_0}} \quad , \; n_1 = \sqrt{\varepsilon_{r_1}}$$

c_1 : speed of light in a medium with arbitry permitivity ε_{r_1} and $\mu_{r_1} = 1$

λ_1 : wavelength of light in a medium with arbitry permitivity ε_{r_1} and $\mu_{r_1} = 1$

k_1 : wavenumber of light in a medium with arbitry permitivity ε_{r_1} and $\mu_{r_1} = 1$ (3.3)

From (3.3), we understand that the refractive index is equal to the square root of the relative permittivity of the medium. Since the fibre material has no magnetic properties, then $\mu_r = 1$ in fibre. This means, the electromagnetic propagation or the guidance of light in fibre will entirely rely on refractive index changes.

Now returning to (3.1), we take the curl of the equation on the first line and benefit from the equation on the second line and the vector identities to write

$$\nabla^2 \mathbf{E} = \mu\varepsilon \frac{\partial^2 \mathbf{E}}{\partial t^2} = \frac{n^2}{c^2} \frac{\partial^2 \mathbf{E}}{\partial t^2} \quad , \quad \nabla^2 \mathbf{E} - \frac{n^2}{c^2} \frac{\partial^2 \mathbf{E}}{\partial t^2} = 0$$

$$\nabla^2 \mathbf{H} = \mu\varepsilon \frac{\partial^2 \mathbf{H}}{\partial t^2} = \frac{n^2}{c^2} \frac{\partial^2 \mathbf{H}}{\partial t^2} \quad , \quad \nabla^2 \mathbf{H} - \frac{n^2}{c^2} \frac{\partial^2 \mathbf{H}}{\partial t^2} = 0 \qquad (3.4)$$

The equations in (3.4) are known as Helmhotz's equations. Our time dependence will be sinusoidal, i.e., $\exp(j\omega t) = \exp(j2\pi f t)$ and the propagation axis, i.e. z dependence will be $\exp(-j\beta z)$, where β is known as the propagation constant (the wave number) of the modes propagating in fibre. Using these and the equivalence of ∇^2 in (3.4), we obtain the following differential equation for the z component of the electric and magnetic fields

$$\frac{\partial^2 E_z}{\partial r^2} + \frac{1}{r}\frac{\partial E_z}{\partial r} + \frac{1}{r^2}\frac{\partial^2 E_z}{\partial \phi^2} + \left(k^2 - \beta^2\right) E_z = 0$$

$$\frac{\partial^2 H_z}{\partial r^2} + \frac{1}{r}\frac{\partial H_z}{\partial r} + \frac{1}{r^2}\frac{\partial^2 H_z}{\partial \phi^2} + \left(k^2 - \beta^2\right) H_z = 0 \qquad (3.5)$$

The other components E_r and E_ϕ , H_r and H_ϕ can be expressed in terms of E_z , and H_z components as shown below.

$$E_r = \frac{1}{j\left(k^2-\beta^2\right)}\left(\beta\frac{\partial E_z}{\partial r}+\frac{\mu\omega}{r}\frac{\partial H_z}{\partial\phi}\right)\ ,\ E_\phi = \frac{1}{j\left(k^2-\beta^2\right)}\left(\frac{\beta}{r}\frac{\partial E_z}{\partial\phi}-\mu w\frac{\partial H_z}{\partial r}\right)$$
$$H_r = \frac{1}{j\left(k^2-\beta^2\right)}\left(\beta\frac{\partial H_z}{\partial r}-\frac{\varepsilon\omega}{r}\frac{\partial E_z}{\partial\phi}\right)\ ,\ H_\phi = \frac{1}{j\left(k^2-\beta^2\right)}\left(\frac{\beta}{r}\frac{\partial H_z}{\partial\phi}+\varepsilon\omega\frac{\partial E_z}{\partial r}\right) \tag{3.6}$$

E_z will have functionally separable dependence on $r,\ \phi,\ z$ and t which can be written as

$$E_z = AF_r(r)F_\phi(\phi)F_z(z)F_t(t) \tag{3.7}$$

where A is a constant to be determined by taking into account the boundary conditions (at core cladding interface). We have already postulated the dependence on z and t in the form of

$$F_z(z)F_t(t) = \exp(-j\beta z)\exp(j2\pi t) \tag{3.8}$$

We further envisage that the dependence on ϕ is also sinusoidal, such that

$$F_\phi(\phi) = \exp(-jv\phi) \tag{3.9}$$

where for completeness v has to be an integer. Thus (3.5) will turn into a differential equation in terms of F_r as stated below

$$\frac{\partial^2 F_r}{\partial r^2}+\frac{1}{r}\frac{\partial F_r}{\partial r}+\left(k^2-\beta^2-\frac{v^2}{r^2}\right)F_r = 0 \tag{3.10}$$

(3.10) is the well known Bessel equation. The solution to (3.10) can be any of the four types of Bessel functions, symbolically denoted as $J_v(x),\ Y_v(x),\ I_v(x),\ K_v(x)$, where v is called the order of the Bessel function, while x is name the argument. We note we have not applied the boundary conditions as yet, so (3.10) covers the propagation both in the core and the cladding. Keeping in mind that propagating modes (physically corresponding to those rays that satisfy the total internal reflection properties) should have finite amplitudes and some oscillatory behaviour, when inside the core and exponential decay from the core cladding interface radially outwards.

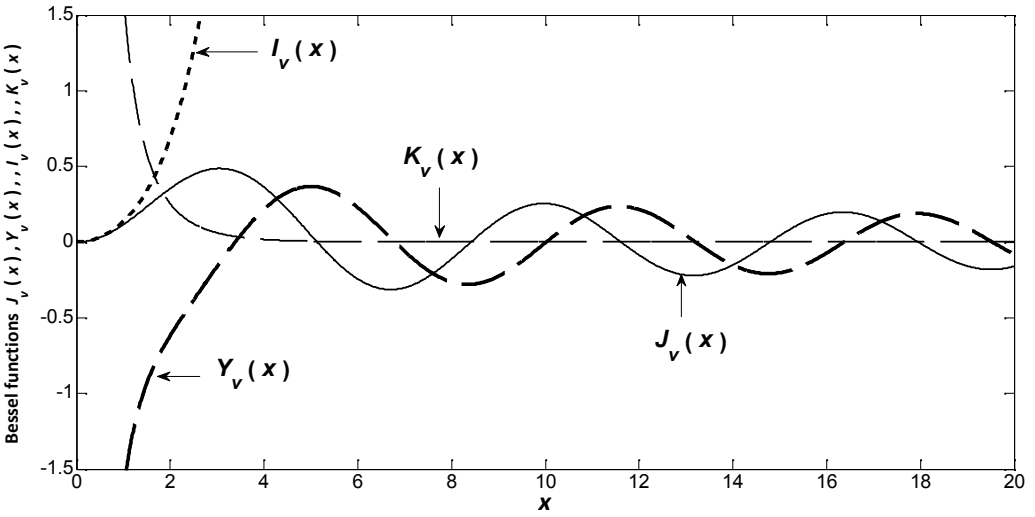

Fig. 3.2 The behaviours of J_v, Y_v, I_v, K_v.

Fig. 3.2 illustrates the behaviours of all possible Bessel functions against the argument, x. In our case this argument will be the radial coordinate r, coupled with some multiplicative factor. In line with the physical interpretation made above for the propagating mode, a suitable choice (from the inspection of the Bessel curves in Fig. 3.2) is the representation of the mode field by J_v inside the core and by K_v inside the cladding. Considering the magnetic field component as well, we can express E_z and H_z fields inside and outside the core as follows

$$\begin{aligned}
&E_z(r<a) = AJ_v(ur)\exp(jv\phi)\exp(j\beta z)\exp(j2\pi t) && \text{inside core}\\
&H_z(r<a) = BJ_v(ur)\exp(jv\phi)\exp(j\beta z)\exp(j2\pi t) && \text{inside core}\\
&E_z(r>a) = CK_v(wr)\exp(jv\phi)\exp(j\beta z)\exp(j2\pi t) && \text{inside cladding}\\
&H_z(r>a) = DK_v(wr)\exp(jv\phi)\exp(j\beta z)\exp(j2\pi t) && \text{inside cladding}
\end{aligned} \qquad (3.11)$$

where B, C, D are new constants and the other newly introduced terms are defined as

$$\begin{aligned}
u^2 &= k_1^2 - \beta^2 \quad , \quad k_1 = \frac{2\pi n_1}{\lambda} = n_1 k\\
w^2 &= \beta^2 - k_2^2 \quad , \quad k_2 = \frac{2\pi n_2}{\lambda} = n_2 k
\end{aligned} \qquad (3.12)$$

Note that the propagation constant β is limited such that

$$k_2 = n_2 k \le \beta \le k_1 = n_1 k \qquad (3.13)$$

In this manner, u^2 and w^2 are always positive or u and w are always real. This is essential for propagating modes. u^2 and w^2 becoming negative corresponds to the case of refracting modes.

Now we come to the application of boundary conditions at $r = a$, i.e. the core cladding boundary. At this boundary, for continuity, we have to match the following fields

$$
\begin{aligned}
&E_z\left(\text{core at } r=a\right)=E_z\left(\text{cladding at } r=a\right)\\
&E_\phi\left(\text{core at } r=a\right)=E_\varphi\left(\text{cladding at } r=a\right)\\
&H_z\left(\text{core at } r=a\right)=H_z\left(\text{cladding at } r=a\right)\\
&H_\phi\left(\text{core at } r=a\right)=H_\varphi\left(\text{cladding at } r=a\right)
\end{aligned}
\tag{3.14}
$$

From the matching conditions of (3.14) and the equalities from (3.6), we get only four constants to be determined from these boundary conditions. These are the constants or the coefficients given in (3.11) and named as A, B, C, D. Here our ait is to find, what is called the characteristic equation, that will yield the propagation constants, i.e. β values of those modes that satisfy the conditions of forward propagation, i.e. propagation to the positive side of the z axis. For this we seek a nontrivial solution to (3.14), which exists if the determinant of the coefficients A, B, C, D are zero. This requirement will deliver the following characteristic equation (CE).

$$
\left[\frac{J_v^{'}(ua)}{uJ_v(ua)}+\frac{K_v^{'}(wa)}{wK_v(wa)}\right]\left[k_1^2\frac{J_v^{'}(ua)}{uJ_v(ua)}+k_2^2\frac{K_v^{'}(wa)}{wK_v(wa)}\right]=\left(\frac{\beta v}{a}\right)\left(\frac{1}{u^2}+\frac{1}{w^2}\right) \tag{3.15}
$$

where prime, ' indicates the derivative of the Bessel function with respect to its argument. By using the following relations

$$
\begin{aligned}
&J_v^{'}(x)=0.5\left[J_{v-1}(x)-J_{v+1}(x)\right] \quad , \quad J_v(x)=0.5\frac{x}{v}\left[J_{v-1}(x)+J_{v+1}(x)\right]\\
&K_v^{'}(x)=-0.5\left[K_{v-1}(x)+K_{v+1}(x)\right] \quad , \quad K_v(x)=0.5\frac{x}{v}\left[K_{v-1}(x)-K_{v+1}(x)\right]
\end{aligned}
\tag{3.16}
$$

It is possible to replace all Bessel function derivatives in (3.15), an act we shall carry out when we write the different versions of CE. Firstly, we examine the case of $v=0$. Here the right hand side of (3.15) becomes zero. Thus we have two CEs separated by the square brackets on the left hand side of (3.15). After using the derivative equivalents given in (3.16), these two CEs will become

$$
\begin{aligned}
&\frac{J_1(u_n)}{u_nJ_0(u_n)}+\frac{K_1(w_n)}{w_nK_0(w_n)}=0 \qquad \text{CE for TE modes}\\
&\frac{k_1^2J_1(u_n)}{u_nJ_0(u_n)}+\frac{k_2^2K_1(w_n)}{w_nK_0(w_n)}=0 \qquad \text{CE for TM modes}
\end{aligned}
\tag{3.17}
$$

where we have used the normalized definitions of, $u_n=ua,\ w_n=wa$. TE mode means that $E_z=0$, while $H_z\neq 0$, i.e. there is no electric field component along the propagation axis. TM mode is defined on the other hand as, $E_z\neq 0$, $H_z=0$. From (3.12), bearing in mind that

$$
k_1=\frac{2\pi n_1}{\lambda} \quad , \quad k_2=\frac{2\pi n_2}{\lambda} \tag{3.18}
$$

The CE given in (3.17) for TM can be converted into

$$\frac{n_1^2 J_1(u_n)}{u_n J_0(u_n)} + \frac{n_2^2 K_1(w_n)}{w_n K_0(w_n)} = 0 \qquad \text{CE for TM modes} \tag{3.19}$$

Finding the zeros (the roots) of the CEs for TE and TM modes will provide us with β values of those modes that will propagate in the fibre. To solve the CEs in (3.17) in this manner, first we remove the singularity in the denominator due to $J_0(u_n)$ by multiplying both sides of the equation by $J_0(u_n)$, hence (3.17) and (3.19) will turn into

$$\frac{n_1^2 J_1(u_n)}{u_n} + \frac{n_2^2 J_0(u_n) K_1(w_n)}{w_n K_0(w_n)} = 0 \;\; , \;\; n_1^2 J_1(u_n) + u_n J_0(u_n) \frac{n_2^2 K_1(w_n)}{w_n K_0(w_n)} = 0 \quad \text{CE for TM modes}$$

$$\frac{J_1(u_n)}{u_n} + \frac{J_0(u_n) K_1(w_n)}{w_n K_0(w_n)} = 0 \;\; , \;\; J_1(u_n) + u_n J_0(u_n) \frac{K_1(w_n)}{w_n K_0(w_n)} = 0 \quad \text{CE for TE modes} \tag{3.20}$$

To generalize the process of finding βs and make this process applicable for any fibre, we define a fibre parameter called normalized frequency, V as follows

$$\begin{aligned}
&u_n = au \;,\; w_n = aw \;,\; \beta_n = a\beta \\
&u_n^2 = a^2 u^2 = a^2\left(k_1^2 - \beta^2\right) = a^2 k_1^2 - \beta_n^2 \\
&w_n^2 = a^2 w^2 = a^2\left(\beta^2 - k_2^2\right) = \beta_n^2 - a^2 k_2^2 \\
&V^2 = u_n^2 + w_n^2 = a^2\left(u^2 + w^2\right) = a^2\left(k_1^2 - k_2^2\right) = a^2 k^2\left(n_1^2 - n_2^2\right) = a^2 k^2 \mathrm{NA}^2
\end{aligned} \tag{3.21}$$

When finding the roots of (3.20), we have to plot of the left hand side of the CEs against two variables, i.e. u_n and w_n. For TM modes, we also need to know (the numeric values of) n_1 and n_2. So in the search for roots of CEs, three dimensional plots will emerge. One sample plot of the CE form TM modes is shown in Fig. 3.3. As seen from this figure, there are several the zero crossings, i.e. the roots, but they are hardly visible. In this sense a contour plot provides a much clearer picture. We combine this contour plot with the first equation on the last line of (3.21), thus obtain what is called V circles. Such combined plot can be found in Fig. 3.4 for the CE of TM modes. As seen from Fig. 3.4, the indices of modes are designated as TM_{vm} where v is the circumfrential mode number (remember that for TE and TM modes, $v = 0$) and m is the order of root. For instance, the first zero crossing (root) is given the index of $m = 1$, while the second root is given the index of $m = 2$ and so on. Thus we see on the graph of Fig. 3.4, the mode labels of TM_{01} and TM_{02}.

Another point of interest is that, since in a fibre, the refractive index difference is much smaller than unity, or $n_1 \simeq n_2$, there s hardly any difference between the zero crossings of TE and TM modes. This means CE of TE modes and CE of TM modes placed on the first and second lines of (3.20) are essentially one single equation. This case is graphically illustrated in Fig. 3.5. It is worth mentioning that the status of $n_1 \simeq n_2$ is named as weak guidance in literature.

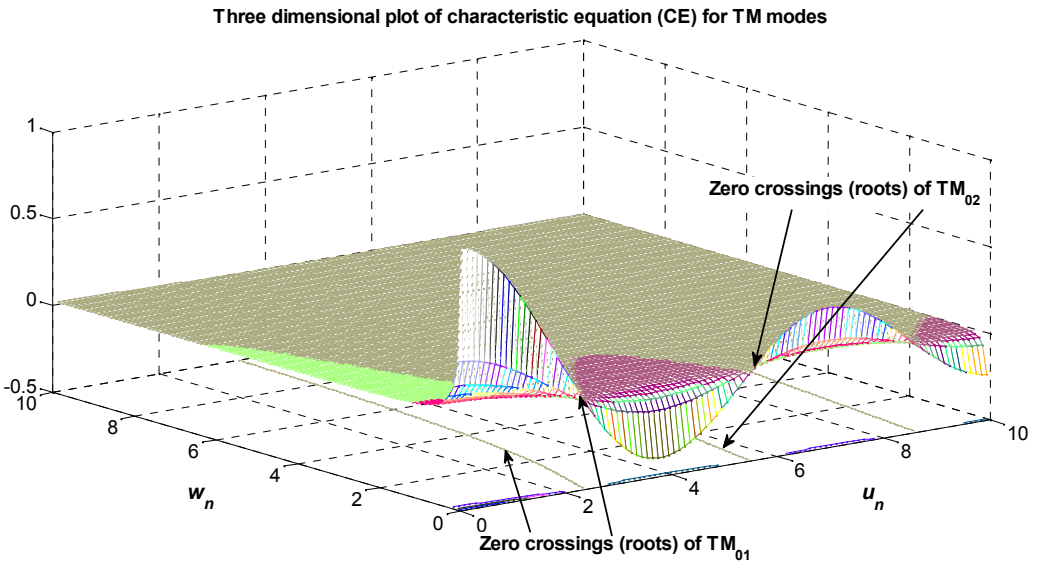

Fig. 3.3 The three dimensional view of the CE for TM modes.

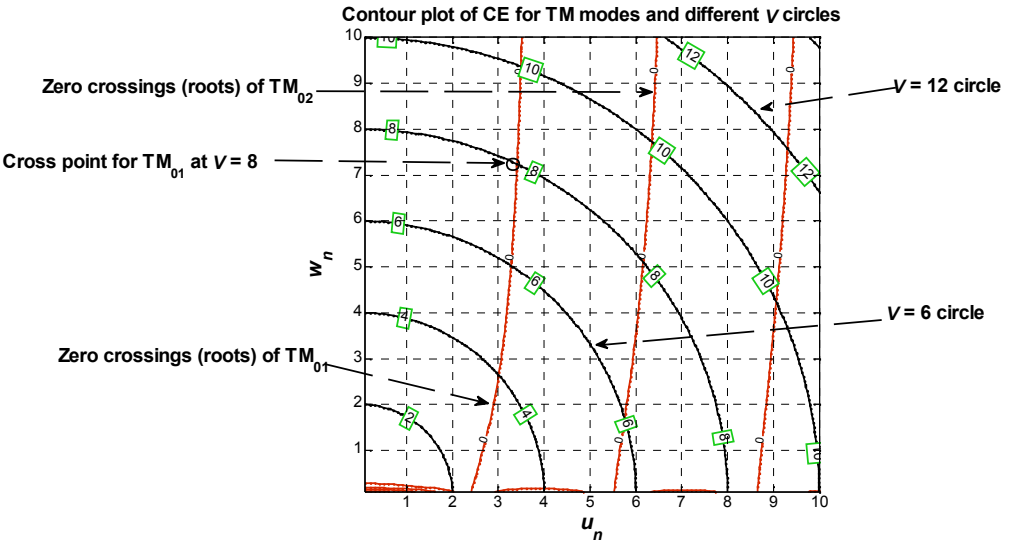

Fig. 3.4 Contour plot of the CE for TM modes and the associated V circles.

Using (3.21), the cross points in Fig. 3.4 can give us the (normalized) propagation constant, i.e. β_n or β of that particular mode at that particular V value. A sample marking is made on Fig. 3.4 for TM_{01} at $V = 8$. Of course to arrive at the actual numeric value of β_n or β, according to (3.21) we need to know the core radius, core refractive index, cladding refractive index or the refractive index difference and the wavelength of the source i.e. a, n_1, n_2 or Δ, λ. In practice, such details can be found on manufacturer's sheet (of course λ depends on our choice of light source). But with the definitions given in (3.12), we are able to treat the propagation in fibres by a single parameter. This means, although there are three separate parameters defining the propagation behaviour of fibre, these are core radius, refractive index difference and the wavelength of operation, they can be combined into a single parameter called normalized frequency parameter. And the propagation characteristics of a fibre can be analysed purely in terms of that normalized frequency parameter.

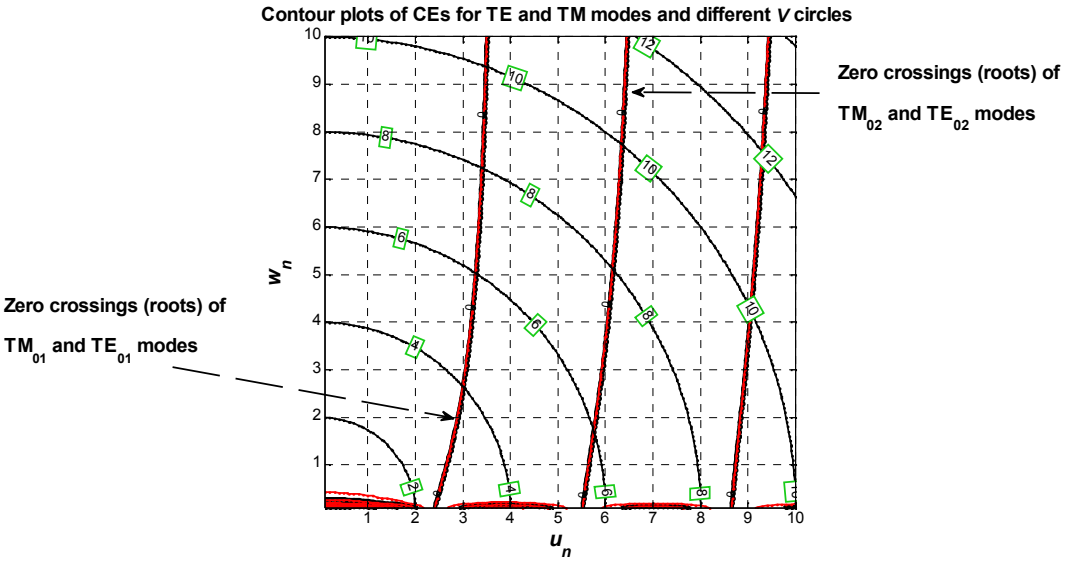

Fig. 3.5 Contour plots of the CE for TE and TM modes and the associated V circles.

Now we return to the general CE given in (3.15) and analyse the case of $v \neq 0$. With this setting, by using (3.16) we obtain

$$\overbrace{\left[\frac{J_{v+1}(u_n)}{u_n J_v(u_n)} + \frac{K_{v+1}(w_n)}{w_n K_v(w_n)}\right]}^{T_1} \overbrace{\left[k_1^2 \frac{J_{v-1}(u_n)}{u_n J_v(u_n)} - k_2^2 \frac{K_{v-1}(w_n)}{w_n K_v(w_n)}\right]}^{T_2}$$
$$+ \overbrace{\left[\frac{J_{v-1}(u_n)}{u_n J_v(u_n)} - \frac{K_{v-1}(w_n)}{w_n K_v(w_n)}\right]}^{T_3} \overbrace{\left[k_1^2 \frac{J_{v+1}(u_n)}{u_n J_v(u_n)} + k_2^2 \frac{K_{v+1}(w_n)}{w_n K_v(w_n)}\right]}^{T_4} = 0 \qquad (3.22)$$

Again plotting (3.22) will give us new zero crossings, new roots and new modes for which the propagation constants can be calculated as explained above. Further simplification can be achieved for the CE of (3.22). That is under the principle of weak guidance, i.e. $n_1 \simeq n_2$ or $k_1 \simeq k_2$. The terms of (3.22) can be approximated as

$$\begin{aligned} &T_4 \simeq k_1^2 T_1 \simeq k_2^2 T_1 \quad , \quad T_2 \simeq k_1^2 T_3 \simeq k_2^2 T_3 \\ &T_1 T_2 + T_3 T_4 \simeq T_1 k_1^2 T_3 + T_3 k_1^2 T_1 \simeq T_1 k_2^2 T_3 + T_3 k_2^2 T_1 \simeq 0 \\ &T_1 T_2 + T_3 T_4 \simeq 2 k_1^2 T_1 T_3 \simeq 2 k_2^2 T_1 T_3 \simeq 0 \quad \rightarrow \quad T_1 T_3 \simeq 0 \end{aligned} \qquad (3.23)$$

The last (approximate) equality means (after converting the approximation into exactness)

$$\left[\frac{J_{v+1}(u_n)}{u_n J_v(u_n)} + \frac{K_{v+1}(w_n)}{w_n K_v(w_n)}\right]\left[\frac{J_{v-1}(u_n)}{u_n J_v(u_n)} - \frac{K_{v-1}(w_n)}{w_n K_v(w_n)}\right] = 0 \qquad (3.24)$$

Setting the first and the second square bracketed terms individually to zero, we get

$$\left[\frac{J_{v+1}(u_n)}{u_n J_v(u_n)}+\frac{K_{v+1}(w_n)}{w_n K_v(w_n)}\right]=0 \qquad \text{CE for EH modes}$$

$$\left[\frac{J_{v-1}(u_n)}{u_n J_v(u_n)}-\frac{K_{v-1}(w_n)}{w_n K_v(w_n)}\right]=0 \qquad \text{CE for HE modes} \qquad (3.26)$$

In order to arrive at the limit of single mode fibre, it is instructive to plot the CEs for HE and HE modes as well. Such a plot can be found in Fig 3.6. We see from Fig. 3.6 that only one mode does not have a cut-off, which means it can theoretically propagate what the V value of the fibre is. That mode is HE_{11} which is the mode chosen for propagate in single mode fibres. Although this mode will continue to exist regardless of fibre V value, for physical reasons, we wish to make the core radius as large as possible to the limit of prevention other modes from propagation. Such a limit can be set by the joint examination of Figs. 3.5 and 3.6. From there and from the horizontal axis of Fig. 3.5, we see that the closest modes to HE_{11} are TE_{01} and TM_{01} which will start to propagate if $V \geq 2.4$. The more exact value is $V \geq 2.45$, which corresponds to the first zero crossing of Bessel function $J_0(x)$. Thus we can say that if we keep the fibre V parameter below the value of 2.45, it will be a single mode fibre.

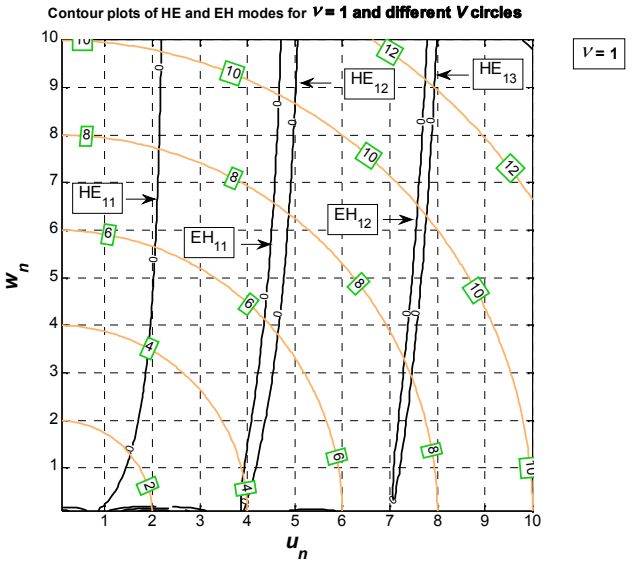

Fig. 3.6 Contour plots of the CE for HE and EH modes and the associated V circles.

As can be noted from (3.26) and Fig. 3.6, it is possible to obtain many modes of EH and HE, since we are at liberty to vary from $v=1$ upwards. But those modes, whose zero crossings (roots) fall outside the V circle of the fibre will not of course propagate, hence we can terminate the process of finding roots from such v values onwards. Below we do an example to illustrate this point.

Example 3.1 : Assume that we have a fibre with $V=4$ and we wish to find which TE and TM modes propagate in this fibre at what propagation constants.

Solution : From Fig. 3.5, we find that $V=4$ circle only encloses the zero crossings (roots) of TE_{01}, TM_{01}. Hence from the point of view of TE and TM modes, only TE_{01}, TM_{01} will propagate in

this fibre. As explained above, the exact numeric value of propagation constants i.e., β_n or β will be determined by the knowledge of other fibre parameters. Assuming, we are dealing with a fibre of $a,\ n_1 = 1.48,\ n_2 = 1.47$ and we use a light source of $\lambda = 1.55\ \mu\text{m}$, then from the last line of (3.21), the core radius to result in a fibre frequency parameter of $V = 4$ is

$$a = \frac{V}{k\left(n_1^2 - n_2^2\right)^{0.5}} = \frac{V}{\frac{2\pi}{\lambda}\left(n_1^2 - n_2^2\right)^{0.5}} = 5.745\ \mu\text{m} \tag{3.27}$$

From Fig. 3.5, we read at the cross point of zero crossings (roots) of TE_{01}, TM_{01} and the $V = 4$ circle, $u_n = 3,\ w_n = 2.6$. Benefiting from (3.21) and (3.27), we can calculate β_n and β as follows

$$\beta_n = \left(a^2k_1^2 - u_n^2\right)^{0.5} = 34.3368 \quad \text{or} \quad \beta_n = \left(a^2k_2^2 + w_n^2\right)^{0.5} = 34.3334$$
$$\beta = \frac{\beta_n}{a} = 5.976\times10^6 \tag{3.28}$$

As a final point, using (3.13), we check that

$$k_2 = n_2k \le \beta \le k_1 = n_1k$$
$$k_2 = 5.9589\times10^6 \quad , \quad \beta = 5.976\times10^6 \quad , \quad k_1 = 5.9994\times10^6 \tag{3.29}$$

Exercise 3.1 : Repeat the calculations in Example 3.1, by switching to $V = 6$ and $V = 10$ and by including HE_{1m} and EH_{1m} from Fig. 3.6. Assume that the larger values of V is obtained by enlarging the core radius.

As an alternative to the displays given in Figs. 3.4 to 3.6 is to plot the variation of the propagation constant or its wavelength and refractive index normalized version against V . Such a graph is given in Fig. 3.7 (copied directly from Fig. 2.5 of Ref. [2], pay attention that in this figure normalized propagation constant is shown by b , below we use the notation b_n , since b is used in these notes to indicate cladding radius).

Here the normalized propagation constant, denoted by b_n is related to the actual propagation constant β as

$$b_n = \frac{\beta/k - n_2}{n_1 - n_2} \tag{3.30}$$

Since in this definition wavelength and the refractive indices are taken into account, we talk about the variation of b_n against V , it effectively means the variations against the core radius, a . As stated in (3.29), for propagating modes β is limited as $n_2k \le \beta \le n_1k$, this way b_n will range between 0 to 1 as shown on the left hand side vertical axis of Fig. 3.7. The vertical axis on the right hand side of Fig. 3.7 is on the other hand marked in the scaling of β/k , named as $\overline{n}$.

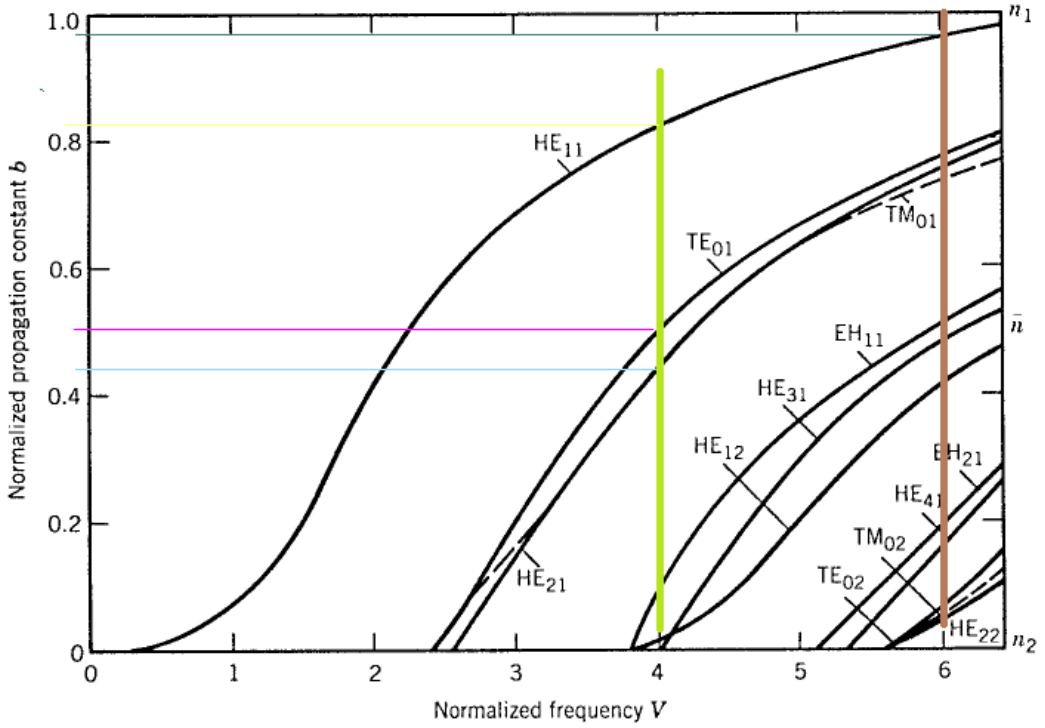

Fig. 3. 7. The variation of normalized propagation constant against the normalized frequency of the fibre for some of the lowest order modes.

Example 3.2 : By adopting the refractive index values and the wavelength of operation, i.e. $n_1 = 1.48,\ n_2 = 1.47,\ \lambda = 1.55\ \mu\text{m}$ find b_n using the formulation given in (3.20) and the plots in Figs. 3.5 and 3.6 at $V = 4$, $V = 6$ and $V = 10$ for $\text{TE}_{01}, \text{TM}_{01}$, HE_{11} and HE_{21} . Compare these calculations with those readings form Fig. 3.7.

Solution : We start with $V = 4$ and $\text{TE}_{01}, \text{TM}_{01}$, because β is calculated in Example 3.1 readily.

$$b_n = \frac{\beta/k - n_2}{n_1 - n_2} \quad \text{inserting} \quad \beta = 5.976\times10^6\ ,\ n_1 = 1.48\ ,\ n_2 = 1.47\ ,\ k = \frac{2\pi}{\lambda} = 4.0537\times10^6$$

$$b_n = \frac{\beta/k - n_2}{n_1 - n_2} = 0.4209 \qquad \text{for } \text{TE}_{01}, \text{TM}_{01} \tag{3.30}$$

Drawing a vertical line in Fig. 3.7, starting at the point of $V = 4$ on the horizontal axis, we find that this vertical line will approximately intersect with $\text{TE}_{01}, \text{TM}_{01}$ curves around $b_n = 0.4209$, that is, the value given on the second line of (3.30). Such action is marked in Fig. 3.7 with coloured lines.

Now we turn to b_n of HE_{11} at $V = 4$. From Fig. 3.6 that the intersection of $V = 4$ circle with HE_{11} curve is at $u_n = 1.914,\ w_n = 3.5$. Again benefiting from (3.21), (3.27), (3.29) and (3.30), we can calculate β and b_n as follows

$$\beta = \frac{\left(a^2 k_1^2 - u_n^2\right)^{0.5}}{a} \quad \text{inserting} \quad a = 5.745 \qquad k_1 = \qquad \times \quad ^6 \quad u_n = \quad 914$$

$$\beta = 5.9507 \times 10^6$$

$$b_n = \frac{\beta / k - n_2}{n_1 - n_2} \quad \text{inserting} \quad \beta = 5.9507 \times 10^6 \ , \ n_1 = 1.48 \ , \ n_2 = 1.47 \ , \ k = \frac{2\pi}{\lambda} = 4.0537 \times 10^6$$

$$b_n = 0.8257 \tag{3.31}$$

Again by following the drawn vertical line in Fig. 3.7, starting at the point of $V = 4$ on the horizontal axis, we find that this vertical line will approximately intersect with HE_{11} curve around $b_n = 0.8257$, that is, the value given on the final line of (3.31).

Now we handle, $V = 6$. For this we recalculate the core radius using (3.27)

$$a = \frac{V}{k\left(n_1^2 - n_2^2\right)^{0.5}} = \frac{6}{4.0537 \times 10^6 \left(1.48^2 - 1.47^2\right)^{0.5}} = 7.5325 \ \mu\mathrm{m} \tag{3.32}$$

From Fig. 3.6, we the intersection of $V = 6$ with HE_{11} curve at $u_n = 2.061, \ w_n = 5.6$, then as in (3.31) β and b_n are calculated as

$$\beta = \frac{\left(a^2 k_1^2 - u_n^2\right)^{0.5}}{a} \quad \text{inserting} \quad a = 7.5325 \qquad k_1 = \qquad \times \quad ^6 \quad u_n = \quad .061$$

$$\beta = 5.9537 \times 10^6$$

$$b_n = \frac{\beta / k - n_2}{n_1 - n_2} \quad \text{inserting} \quad \beta = 5.9537 \times 10^6 \ , \ n_1 = 1.48 \ , \ n_2 = 1.47 \ , \ k = \frac{2\pi}{\lambda} = 4.0537 \times 10^6$$

$$b_n = 0.8825 \tag{3.33}$$

We again see that, the value of $b_n = 0.8825$ agrees well with the value read from the left side of the vertical axis in Fig. 3.7. The case of other modes at $V = 6$ is left as lab exercise.

It is interesting to find a simple relationship between b_n and V for HE_{11} curve. This is given by

$$b_n(V) \simeq \left(1.1428 - 0.996 / V\right)^2 \tag{3.34}$$

which is known to be accurate within 0.2 % for V in the range 1.5-2.5, the range where most practical single mode fibres lie in.

4. Single Mode Fibres

As mentioned above and as seen from Fig. 3.6, only one mode, namely HE_{11} is free from cut off, i.e. it propagates regardless of the V value. This means that HE_{11} will continue to propagate even when, the V approaches zero, which corresponds to having core radius, assuming finite wavelength and refractive index difference. Of course have a fibre of nearly zero radius would create practical problems, such as alignment, handling etc. Therefore to obtain single mode fibre, we seek the largest

value of V , yet eliminate the other modes. Looking at Fig. 3.5, we see that, modes closest HE_{11} are TE_{01} and TM_{01}. Hence it will be sufficient to set V just below the cut off values of TE_{01} and TM_{01}, that is $V \leq 2.45$. From (3.17) and (3.20), this is the first root (the zero crossing) of $J_0(u_n = 2.45)$, when $w_n = 0$.

After suppressing the time variations, by using (3.6), (3.7) and (3.11), the radial component of the single mode can be written as

$$E_r = \begin{cases} \dfrac{J_0(ur)}{J_0(u_n)}\exp(j\beta z) = \dfrac{J_0(u_n r_n)}{J_0(u_n)}\exp(j\beta z) \quad , \quad r_n = r/a \quad r < a \quad \text{inside core} \\ \dfrac{K_0(wr)}{K_0(w_n)}\exp(j\beta z) = \dfrac{K_0(w_n r_n)}{K_0(w_n)}\exp(j\beta z) \qquad\qquad r > a \quad \text{inside cladding} \end{cases} \tag{4.1}$$

It is possible to plot the radial component of the electric field, using formulation given in (4.1). This is shown in Fig. 4.1.

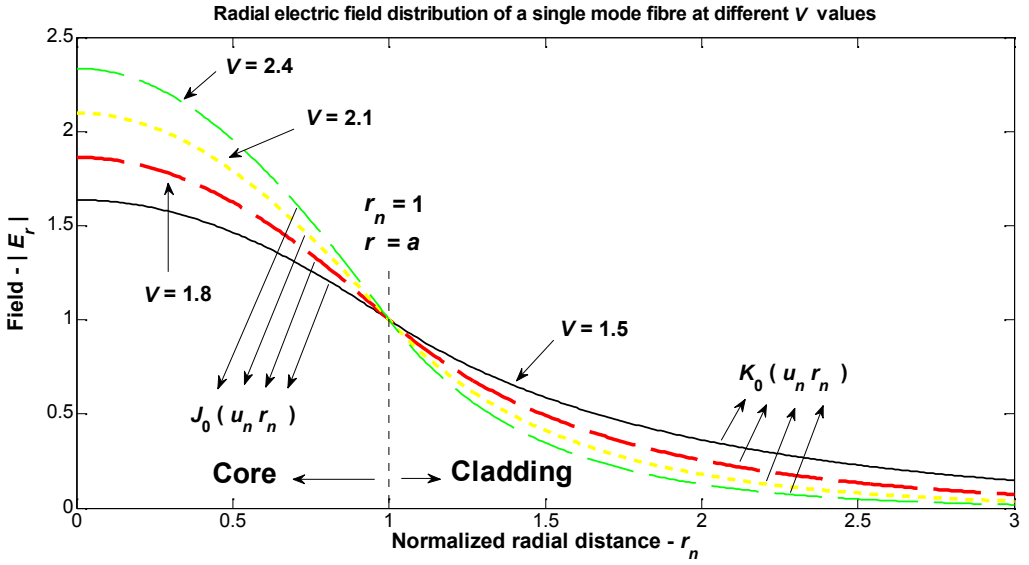

Fig. 4.1 The radial electric field distribution of HE_{11} in a single mode fibre at different V values.

Quite a number of observations are possible regarding Fig. 4.1. They are listed below.

- The field in a single fibre distributes itself more or less evenly between the core and the cladding. This is in contrast to the propagating modes of the multimode fibre where the field decays considerably before the core cladding boundary. But in a single mode fibre, as seen from Fig. 4.1, an important portion of the field propagates in the cladding region and this portion increases in inverse proportionality with V values. For this reason illustrated in Fig. 4.1 and to minimize alignment problems, we tend to operate at V values (of course we must bear in mind that in all cases, we cannot exceed $V = 2.45$).
- In a single mode fibre, cladding material has to be high quality (in addition to the core), due to the existence of a sizable portion of the field in the cladding. This means that a constant refractive

index value, n_2 must be maintained uniformly along the radial, circumferential and axial directions, at least in the regions of close proximity to the core cladding boundary.

- Inside the core, field distribution is governed by the Bessel function, $J_0\left(u_n r_n\right)$, while this is handed over to the Bessel function $K_0\left(w_n r_n\right)$ inside the cladding. Thanks to the boundary matching conditions applied in (3.14), there is perfect continuity between the two fields at the core cladding boundary, that is $r_n = 1$ or $r = a$.

Note that in Fig. 4.1 variation of V (or the fibre variation) is actually achieved by changing the core radius, yet the horizontal axis is normalized with respect to the core radius of each fibre separately and is common to all curves. In this manner, if the plot of the radial field for each fibre was along its own absolute radial distance axis, the part of the field in the core and the cladding would change somewhat. This fact does not alter the essence of above observations.

When a cross section of the single mode fibre is viewed, the illumination created by HE_{11} mode will look like the image given Fig. 4.2. As we see from this figure, the central part of the core area is highly illuminated, but as we move to the cladding the, light intensity reduces.

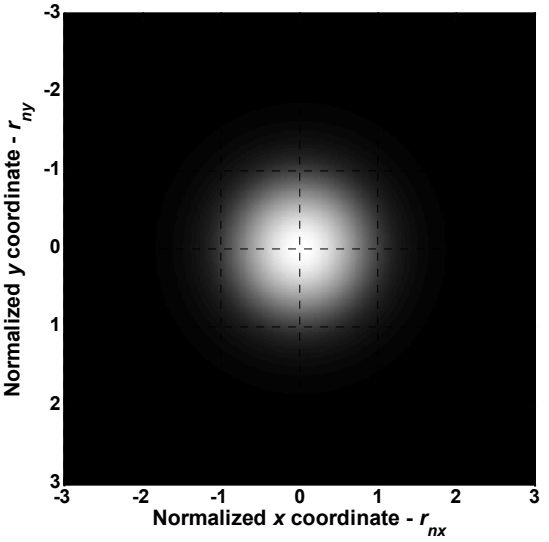

Fig. 4.2 Light illumination of HE_{11} mode in a single mode fibre of $V = 2$.

It is possible to gather and approximate the core and the cladding parts of the radial field of (4.1) under a single Gaussian exponential as expressed below

$$E_r \simeq A \exp\left(-\frac{r_n^2}{w_s^2}\right) \exp\left(j\beta z\right) \tag{4.2}$$

where w_s is known as the spot size determining basically how much the field is confined to the core or how much it extends into the cladding. An approximate relation between w_s and V exists and it valid in the range $1.2 < V < 2.4$ and is given by

$$w_s \simeq 0.65 + 1.619V^{-1.5} + 2.879V^{-6} \tag{4.3}$$

By choosing several V values, in Figs. 4.3 and 4.4, we try to illustrate how close (4.2) models the two part field expression of (4.1).

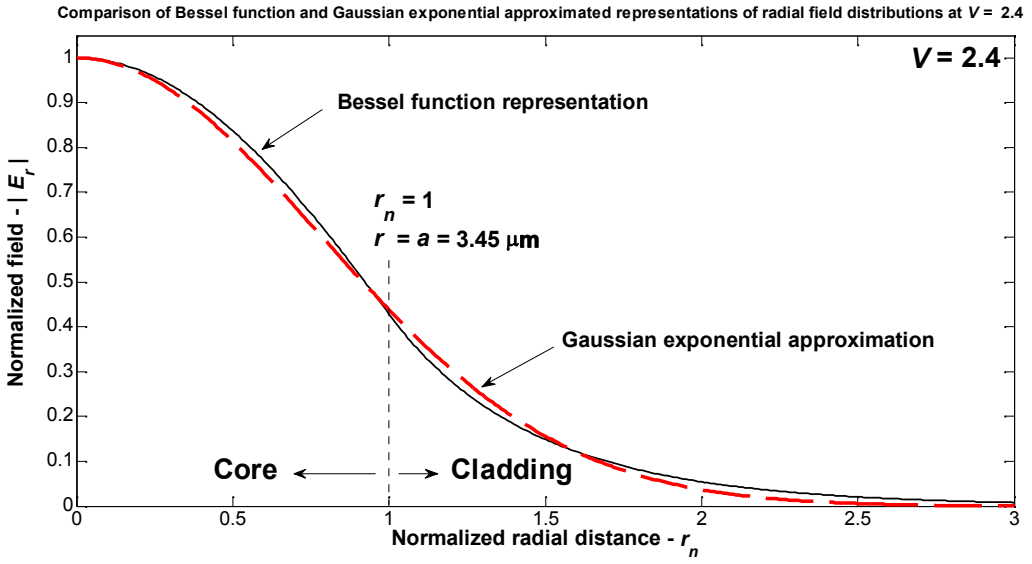

Fig. 4.3 Bessel function representation and the Gaussian exponential approximation of the radial field in a single mode fibre at $V = 2.4$.

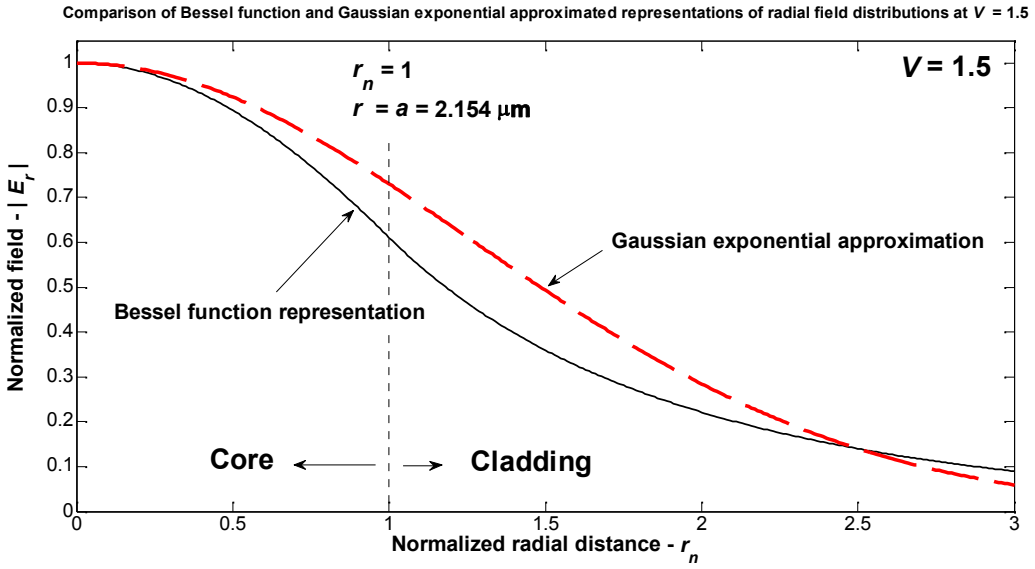

Fig. 4.4 Bessel function representation and the Gaussian exponential approximation of the radial field in a single mode fibre at $V = 1.5$.

Here the separate figures for $V = 2.4$ and $V = 1.5$ are chosen because of the common axis problem mentioned above. Consequently, the normalized horizontal axis of Figs. 4.3 and 4.4 are according to the core radius values given in these figures. Additionally in both figures, the amplitude of the field (i.e. the vertical axis) for Bessel function representation is also normalized with respect to its peak in order to get a meaningful comparison between Bessel function representation of (4.1) and the

Gaussian exponential approximation of (4.3). Comparing Figs. 4.3 and 4.4, we see that at larger V values, the Gaussian exponential approximation of (4.3) is indeed a close match to the Bessel function representation of (4.1). But as V is reduced, the difference between the two curves seems to increase as displayed in Fig. 4.4. But this is considered to be major problem, since most practical fibres are operated closer to $V = 2.4$.

Finally on single mode fibres, we calculate the percentage of mode power contained inside the core. For this we take (4.2) and define a confinement factor, Γ_c as follows

$$\Gamma_c = \frac{P_{core}}{P_{total}} = \frac{\int_0^1 |E_r|^2 \, dr_n}{\int_0^\infty |E_r|^2 \, dr_n} = \frac{\int_0^1 \exp\left(-\frac{2r_n^2}{w_s^2}\right) dr_n}{\int_0^\infty \exp\left(-\frac{2r_n^2}{w_s^2}\right) dr_n} = 1 - \exp\left(-\frac{2}{w_s^2}\right)$$

$$= 1 - \exp\left[-\frac{2}{\left(0.65 + 1.619V^{-1.5} + 2.879V^{-6}\right)^2}\right] \qquad (4.4)$$

where on the last line of (4.4), we have used the V equivalence of w_s given in (4.3).

In Fig. 4.5, Γ_c is plotted against V.

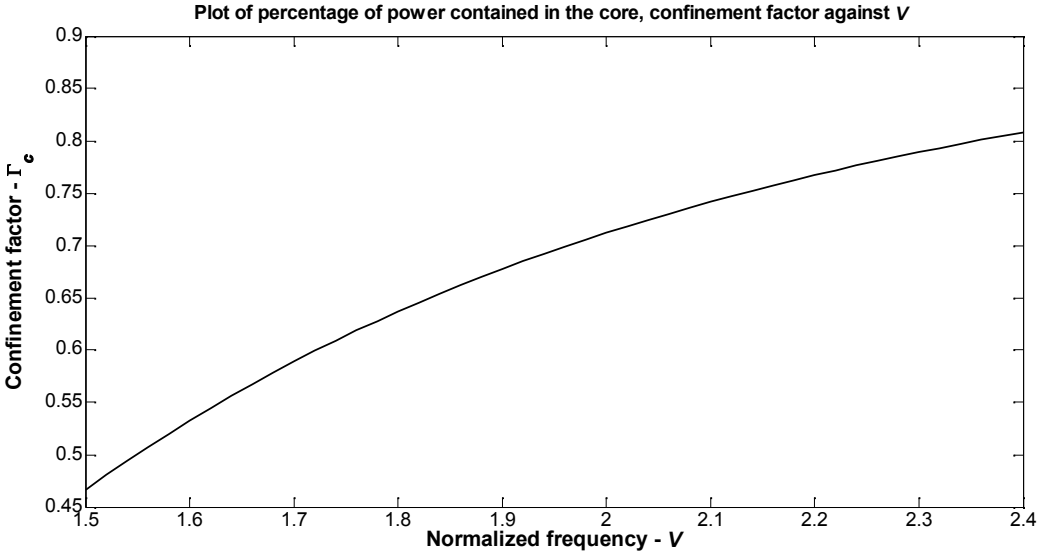

Fig. 4.5 Plot of confinement factor showing the percentage of power contained in the core during propagation in single mode fibre.

According to Fig. 4.5, just above 80 % of power of the HE_{11} mode will be contained in the core when $V = 2.4$, but this percentage drops as the value of V is lowered.

These notes are based on

1) Gerd Keiser, “Optical Fiber Communications” 3nd Ed. 2000, McGraw Hill, ISBN : 0-07-116468-5.
2) Govind P. Agrawal, “Fiber-Optic Communication Systems” 2002, Jon Wiley and Sons, ISBN : 0-471-21571-6.
3) B. E. A. Saleh, M.C. Teich “Fundamentals of Photonics” , 2007, Wiley, ISBN No : 978-0-471-35832-9.
4) My own ECE 474 Lecture Notes.